provides a clean signature: $pp \to HK^+K^+$. The H itself need not be seen since any mass less than 2230 MeV recoiling against two positive kaons would be unambiguous. Either a bubble-chamber or counter experiment is possible. This process has the further advantage of mapping out the $\Lambda\Lambda$ mass spectrum whether or not the H (and/or H^*) is found.

Other possible production mechanisms include $\Lambda p \to HK^+$, $\Sigma^- p \to HK^0$, $\Xi^- p \to H\pi^0$, $K^- d \to HK^0$, and $K_L d \to HK^+$. Any mechanism involving neutral kaons admits a large dineutron background because of K^0-$\bar{K}^0$ mixing.

The dynamics of the H^* are similar to those of the H in the mass range of case (3). We expect it to show itself as a bump in $\Lambda\Lambda$ invariant-mass plots at approximately 2335 MeV.

At present, data on dihyperon channels are meager. Low-statistics dilambda mass spectra[10] seen in Ξ^- or K^- capture on nuclei show one or two bumps below the $\Sigma\Sigma$ threshold. Nuclear rescattering effects tend to wash out any structure. At least one[11] and perhaps another[12] doubly strange hypernuclei are known from emulsion experiments. In these events, a Ξ is apparently captured on a light emulsion nucleus causing it to fragment into an ordinary nucleus and a double hyperfragment (e.g., ${}_{\Lambda\Lambda}\mathrm{He}^6$) which is identified by successive emission of π^- as the two Λ's decay. If the two hyperons were bound as an H in the nucleus, double π decay would be forbidden [$M(H) < 2193$ MeV] or at least inhibited [$M(H) > 2193$ MeV]. Either $M(H) > 2193$ MeV or nuclear effects are such that at least one Λ decays before reacting to form an H. Further experiments on proton (or deuteron) targets are necessary to settle the matter.

I would like to thank J. Bjorken, S. D. Drell, F. Gilman, V. Hepp, and P. Mannheim for helpful discussions.

*Supported in part through funds provided by the U. S. Energy Research and Development Administration under Contracts No. AT(11-1)3069 and No. E(04-3)-515.

†A. P. Sloan Foundation Fellow on leave from Massacusetts Institute of Technology.

‡Present address.

[1]R. F. Dashen, in *Proceedings of the International Symposium on Lepton and Photon Interactions at High Energies, Stanford, California, 1975*, edited by W. T. Kirk (Stanford Linear Accelerator Center, Stanford, Calif., 1975).

[2]A. Chodos, R. L. Jaffe, K. Johnson, C. B. Thorn, and V. F. Weisskopf, Phys. Rev. D 9, 3471 (1974).

[3]T. DeGrand, R. L. Jaffe, K. Johnson, and J. Kiskis, Phys. Rev. D 12, 2060 (1975).

[4]R. L. Jaffe, Phys. Rev. D (to be published).

[5]R. L. Jaffe, Phys. Rev. D (to be published).

[6]O. I. Dahl *et al.*, Phys. Rev. Lett. 6, 142 (1961); D. Cline *et al.*, Phys. Rev. Lett. 20, 1452 (1968); V. Hepp, in Proceedings of the Baryon Resonance Conference, Oxford, England, July 1976 (to be published).

[7]R. J. Oakes, Phys. Rev. 131, 2239 (1963).

[8]A. de Rújula, H. Georgi, and S. L. Glashow, Phys. Rev. D 12, 147 (1975).

[9]For a discussion of a model of the nucleon-nucleon force based on this picture, see C. de Tar, MIT Report No. MIT-CTP-546, 1976 (to be published).

[10]P. Beillière *et al.*, Phys. Lett. 39B, 671 (1972); B. A. Shahbazian and A. A. Timonina, Nucl. Phys. B53, 19 (1973), other references cited therein.

[11]D. Prowse, Phys. Rev. Lett. 17, 782 (1966).

[12]M. Danysz *et al.*, Phys. Rev. Lett. 11, 29 (1963), and Nucl. Phys. 49, 121 (1963).

$\eta\gamma$ Decays of ρ^0, ω, and φ Mesons*

D. E. Andrews,† Y. Fukushima, J. Harvey, F. Lobkowicz, E. N. May, C. A. Nelson, Jr., and E. H. Thorndike
Department of Physics and Astronomy, University of Rochester, Rochester, New York 14627
(Received 3 November 1976)

$\eta\gamma$ decays of ρ^0, ω, and φ are studied. We find $\Gamma(\varphi \to \eta\gamma) = 55 \pm 12$ keV. Our data admit two solutions for $(\rho^0, \omega) \to \eta\gamma$: Either $\Gamma(\rho^0 \to \eta\gamma) = 50 \pm 13$ keV, $\Gamma(\omega \to \eta\gamma) = 3.0^{+2.5}_{-1.8}$ keV, and the $(\omega, \rho) \to \eta\gamma$ relative decay phase is near zero; or $\Gamma(\rho^0 \to \eta\gamma) = 76 \pm 15$ keV, $\Gamma(\omega \to \eta\gamma) = 29 \pm 7$ keV, and the decay phase is near 180°.

The desire to apply theoretical ideas about radiative decays to the new mesons, coupled with a disagreement between these ideas and recent measurements[1-3] of $\varphi \to \eta\gamma$, $\rho \to \pi\gamma$, and $K^* \to K\gamma$ partial widths, has led to heightened interest in vector-meson radiative decays. Experimental information of these processes is incomplete—only five of the ten radiative widths between the vector

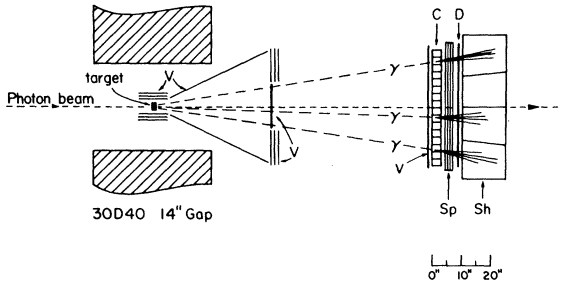

FIG. 1. Plan view of experiment.

and pseudoscalar nonets are known, and most of these are known rather poorly. In this Letter, we report a first measurement of $\rho^0 \to \eta\gamma$, an improved measurement of $\varphi \to \eta\gamma$, and information on $\omega \to \eta\gamma$.

The vector mesons whose decays we observed were produced by diffractive photoproduction from a complex-nucleus target, with use of the tagged photon beam of the Wilson Synchrotron Laboratory at Cornell University. Diffractive photoproduction is a well-understood production mechanism, with features that allow good rejection of background processes. The experimental layout is shown in Fig. 1. A 6.7–10.2-GeV tagged photon beam (200-MeV tag bins) is incident on a 0.1-radiation-length copper target. Diffractively photoproduced vector mesons undergoing radiative decays $V \to P\gamma$ and $P \to \gamma\gamma$ result in final states consisting of three γ rays. The γ rays pass through a magnetic field and anticoincidence counters (V), and are then converted in a 32-element array of 3.5-radiation-length–thick lead-glass shower counters (C). Shower positions are measured by magnetostrictive readout strip spark chambers (Sp). The showers pass through an array of scintillation counters (D), used in the trigger and for timing, and enter a 16-element, lead-perchlorate–filled Cherenkov shower counter (Sh). Decay photon energies are obtained by summing energies deposited in the appropriate elements of the thin lead-glass counters and thick lead perchlorate counters. The system determines γ-ray energies to $\pm 15\%/(E_{\mathrm{GeV}})^{1/2}$, rms, and γ-ray positions to ± 0.26 in., rms. An array of anticoincidence counters (V) limits the final data sample to events containing only neutral, forward particles.

The hardware trigger for the experiment is quite loose, requiring a tagged photon, three or more γ-ray candidates, at least 4-GeV energy deposited, and no forward charged particles. In analysis, we require further that there be exactly

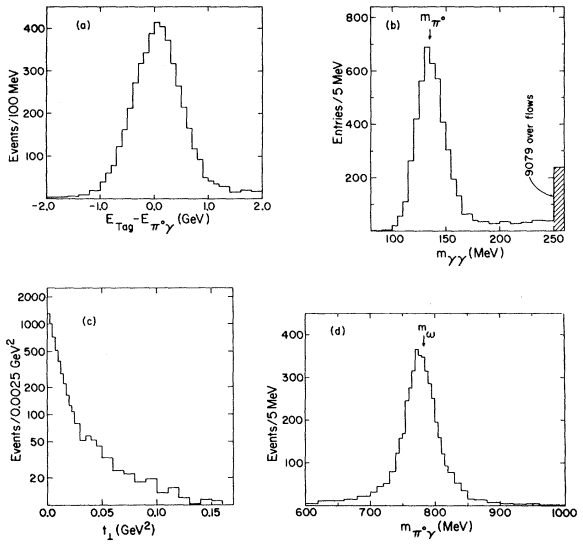

FIG. 2. Distributions for diffractive, elastic $\omega \to \pi^0\gamma$ candidates. (a) Elasticity distribution for small-$t_\perp$ events satisfying π^0- and ω-mass cuts. (b) $\gamma\gamma$ mass spectrum for elastic, small-$t_\perp$ events satisfying an ω-mass cut. (c) $t_\perp$ distribution for elastic events satisfying π^0- and ω-mass cuts. (d) $\pi^0\gamma$ mass spectrum for small-$t_\perp$ elastic events satisfying a π^0-mass cut.

three γ rays, no energy deposited in C or Sh not associated with these three γ rays, no spurious tracks in Sp, and no V counter coincidence. For additional rejection of background, two features of diffractive photoproduction on a complex nucleus are utilized: (a) The process is elastic; hence, the energy of the 3γ system should equal that of the incident tagged photon; (b) the process is sharply forward-peaked, behaving like $\exp(-170t_\perp)$ for copper.

The well-established $\omega \to \pi^0\gamma$ decay dominates the diffractive, elastic signal, and is useful for calibration, normalization, and tests. The elasticity distribution of small-$t_\perp$ $\omega \to \pi^0\gamma$ events, the $\gamma\gamma$ mass spectrum for small-$t_\perp$ elastic ω events, the $t_\perp$ distribution of elastic $\omega \to \pi^0\gamma$ events, and the $\pi^0\gamma$ mass distribution for small-$t_\perp$ elastic events are shown in Figs. 2(a)–2(d) (with $t_\perp \equiv p_\perp^2$). In these distributions, resolution has been improved by imposing elasticity as a constraint in Figs. 2(b)–2(d), and by imposing the π^0 mass as a constraint in Figs. 2(c) and 2(d). Note the expected features: elastic peak, π^0 mass peak, forward diffractive peak, and ω mass peak. The peak locations and widths are in accord with expectations, demonstrating that our calibrations are correct and our resolutions are understood.

From the $\omega \to \pi^0\gamma$ signal just discussed and the

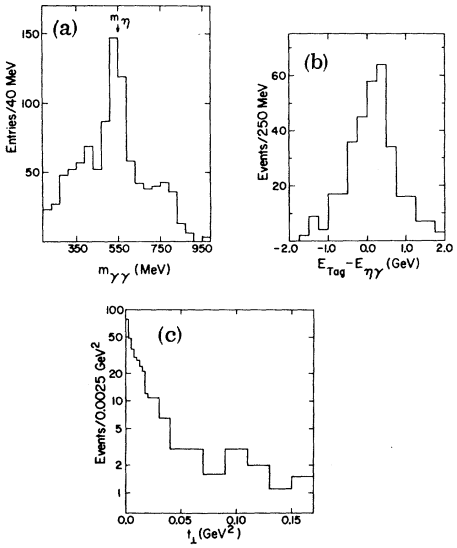

FIG. 3. Distributions for non-π^0 events. (a) $\gamma\gamma$ mass spectrum for small-$t_\perp$ elastic events (three combinations/event). (b) Elasticity distribution for small-$t_\perp$ $\eta\gamma$ events. (c) $t_\perp$ distribution for elastic $\eta\gamma$ events. Acceptance, not corrected for, is flat in $t_\perp$ and slowly varying in elasticity.

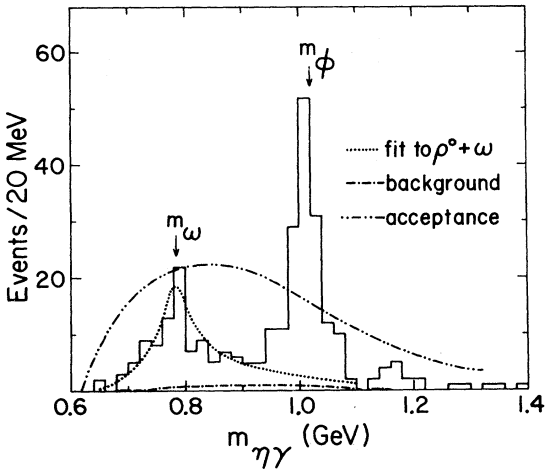

FIG. 4. $\eta\gamma$ mass distribution of small-$t_\perp$, elastic, non-π^0 events. The fit (dotted curve) is described in the text.

known[4] $\omega \to \pi^0\gamma$ branching ratio, one can obtain the $\gamma Cu \to \omega Cu$ forward cross section. We obtain[5] 11.4 ± 1.0 mb/GeV^2, which compares well with 10.4 ± 0.8 mb/GeV^2, the average of the two experiments[6] studying ω photoproduction through its dominant decay, $\pi^+\pi^-\pi^0$.

To study $\eta\gamma$ decays, it is necessary to impose a π^0 anticut, since π^0's dominate the 3γ events and η's are relatively rare. In Fig. 3(a), we show the 2γ mass spectrum of small-$t_\perp$ elastic events for which no 2γ mass combination is below 200 MeV. For each event, three combinations are plotted. An η peak is apparent. Indeed two thirds of all events plotted have one combination within the η peak. Imposing an η-mass cut, we display in Figs. 3(b) and 3(c) an elasticity distribution for small-$t_\perp$ events, and a $t_\perp$ distribution for elastic events. The signal shows the characteristics expected—elastic peak and diffractive peak. [In these plots, elasticity has been imposed as a constraint in Figs. 3(a) and 3(c), while the η mass has been imposed as a constraint in Fig. 3(c).]

The $\eta\gamma$ mass spectrum of small-$t_\perp$ elastic events is shown in Fig. 4. Acceptance has not been corrected for; it is shown on Fig. 4. In obtaining this plot, kinematic cuts and constraints have been imposed in the following order: (a) Events with any $\gamma\gamma$ mass combination below 200 MeV were cut, as potential π^0 events; (b) an elasticity cut of ± 1 GeV was made; (c) elasticity was imposed as a constraint; (d) events not having at least one $\gamma\gamma$ mass combination between 0.47 and 0.63 GeV were cut, as not being η events; (e) the η mass was imposed as a constraint; and (f) events with $t_\perp > 0.02$ GeV^2 were cut. With this procedure, the $\eta\gamma$ mass resolution is $\pm 1.7\%$ rms. Figure 4 shows a clean $\varphi \to \eta\gamma$ signal, and a region containing $(\rho^0, \omega) \to \eta\gamma$. From Fig. 3, there is every indication that the background to $V \to \eta\gamma$ events in Fig. 4 is quite small. This is confirmed by extrapolating the large-$t_\perp$ mass spectrum ($0.1 \leq t_\perp \leq 0.2$) to small $t_\perp$. The background obtained in this way is shown on Fig. 4, and is unimportant. In the following, we make the plausible assumption that nonresonant diffractive, elastic processes are small, and can be neglected.

Extraction of the $\varphi \to \eta\gamma$ partial width from Fig. 4 is straightforward. Normalizing against the number of $\omega \to \pi^0\gamma$ events in Fig. 2(d), using a Monte Carlo simulation to determine the relative detection efficiencies, taking 0.40 ± 0.08 for the ratio of φ- to ω-photoproduction cross sections on copper,[6,7] and using accepted[4] values for the $\omega \to \pi^0\gamma$ branching ratio and the φ total width, we obtain[8] $R(\varphi \to \eta\gamma) = (1.35 \pm 0.29)\%$ and $\Gamma(\varphi \to \eta\gamma) = 55 \pm 12$ keV.

To extract $\rho^0 \to \eta\gamma$ and $\omega \to \eta\gamma$ from the data, one must take into account the fact that ρ^0 and ω overlap, and because the production mechanism is the same in both cases, the two processes are fully coherent and interfere. We analyze the 0.60—0.94-GeV region of the $\eta\gamma$ mass spectrum with

a maximum-likelihood method, describing both ρ^0 and ω by Ross-Stodolsky-modified relativistic p-wave Breit-Wigner functions. There are three fitting parameters: $R(\rho^0 \to \eta\gamma)$, $R(\omega \to \eta\gamma)$, and Φ, the phase by which the ω amplitude leads the ρ^0 amplitude. This relative phase is a sum of the relative production phase (expected to be near zero, for similar production mechanisms) and the relative decay phase (expected to be near zero or 180°, by time-reversal-invariance arguments). That portion of the phase due to the Breit-Wigner functions has been removed.

We find two equally good solutions—one resulting from constructive interference and the other from destructive interference; their fit is shown on Fig. 4. The constructive-interference solution[5,9] is $R(\rho \to \eta\gamma) = (3.6 \pm 0.9) \times 10^{-4}$, $\Gamma(\rho \to \eta\gamma) = 50 \pm 13$ keV, $R(\omega \to \eta\gamma) = (3.0^{+2.5}_{-1.8}) \times 10^{-4}$, $\Gamma(\omega \to \eta\gamma) = 3.0^{+2.5}_{-1.8}$ keV, and $\Phi = -11° \pm 38°$. The destructive-interference solution[5,9] is $R(\rho \to \eta\gamma) = (5.4 \pm 1.1) \times 10^{-4}$, $\Gamma(\rho \to \eta\gamma) = 76 \pm 15$ keV, $R(\omega \to \eta\gamma) = (29 \pm 7) \times 10^{-4}$, $\Gamma(\omega \to \eta\gamma) = 29 \pm 7$ keV, and $\Phi = 203° \pm 10°$. The errors quoted above allow for correlations among the three quantities. For the constructive-interference solution, there are strong correlations between the two partial widths, and an appropriately chosen linear combination can be determined more accurately than either width separately. Specifically, we find $\Gamma(\rho \to \eta\gamma) + 3\Gamma(\omega \to \eta\gamma) = 59 \pm 12$ keV (constructive-interference case).

Our value for $\Gamma(\varphi \to \eta\gamma)$ agrees well with the Orsay storage ring measurement[1] of 62 ± 16 keV. Both are considerably below the simple quark-model prediction[10] of 340 keV. The quark model predicts a relative phase of zero for the $\rho \to \eta\gamma$ and $\omega \to \eta\gamma$ decay amplitudes, and further predicts $\Gamma(\rho \to \eta\gamma) = 50$ keV, $\Gamma(\omega \to \eta\gamma) = 6.3$ keV, and $\Gamma(\rho \to \eta\gamma) + 3\Gamma(\omega \to \eta\gamma) = 69$ keV. All this is in good agreement with our constructive-interference solution.

Of the very large number of recent theoretical papers on vector-meson radiative decays, those[11] in reasonable agreement with both the $\varphi \to \eta\gamma$ and the $(\rho^0, \omega) \to \eta\gamma$ results all predict $\Gamma(\rho \to \pi\gamma)$ to be in the 70–100 keV range, in conflict with experiment.[2]

We thank Professor B. D. McDaniel for the hospitality shown us by the Laboratory for Nuclear Studies during the course of this experiment. Mr. Thomas Miller assisted us during the early stages of this experiment.

---

*Research supported by the National Science Foundation.

†Present address: Laboratory of Nuclear Studies, Cornell University, Ithaca, N. Y. 14853.

[1]G. Cosme *et al.*, Phys. Lett. 63B, 352 (1976).

[2]B. Gobbi *et al.*, Phys. Rev. Lett. 33, 1450 (1974).

[3]W. C. Carithers *et al.*, Phys. Rev. Lett. 35, 349 (1975).

[4]T. G. Trippe *et al.*, Rev. Mod. Phys. 48, No. 2, Pt. 2, S51 (1976).

[5]Because $\rho^0 \to \pi^0\gamma$ is present and interferes with $\omega \to \pi^0\gamma$, a correction is required. We use $\Gamma(\rho \to \pi\gamma) = 35$ keV, from Ref. 2, in making this correction. For a different $\rho^0 \to \pi^0\gamma$ radiative width, the ω photoproduction cross section should be divided by $\{0.87 + 0.13[\Gamma(\rho \to \pi\gamma)/35 \text{ keV}]^{1/2}\}$. Similarly, all $\eta\gamma$ branching ratios and radiative widths should be multiplied by this factor.

[6]H.-J. Behrend *et al.*, Phys. Rev. Lett. 24, 1246 (1970); J. Abramson *et al.*, Phys. Rev. Lett. 36, 1428 (1976).

[7]G. McClellan *et al.*, Phys. Rev. Lett. 26, 1593 (1971).

[8]We have omitted a correction due to interference of $\rho^0 \to \eta\gamma$ with $\varphi \to \eta\gamma$, which we estimate to be ± 5%, using our fitted $\rho^0 \to \eta\gamma$ and $\varphi \to \eta\gamma$ partial widths, information about the ρ^0-φ relative production phase from photoproduction studies, and the fact that the ρ^0-φ relative decay phase is real, by time reversal. The sign of the correction depends on whether the decay phase is 0° or 180°.

[9]In obtaining these values, we have again normalized against the number of $\omega \to \pi^0\gamma$ events. We use 12 ± 1.8 for the ratio of ρ^0- to ω-photoproduction cross sections on copper (Ref. 6), and use 140 and 10 MeV for the ρ^0 and ω total widths.

[10]R. VanRoyen and V. F. Weisskopf, Nuovo Cimento 50A, 617 (1967).

[11]Etim-Etim and M. Greco, CERN Report No. Th. 2174-CERN, 1976 (to be published); G. J. Gounaris, Phys. Lett. 63B, 307 (1976); A. Kazi, G. Kramer, and D. H. Schiller, Acta Phys. Austriaca 45, 195 (1976).